

The Impact of FDM Process Parameters on the Compression Strength of 3D Printed PLA Filaments for Dental Applications

Mostafa Adel Hamed^{1*}, Tahseen Fadhil Abbas¹

¹ Metallurgical Engineering and Production Department, University of Technology, Baghdad, Iraq

* Corresponding author's e-mail: mostafa.a.hamed@uotechnology.edu.iq

ABSTRACT

This study evaluated Fused Deposition Modeling (FDM) for printing objects with maximum compression strength by focusing on critical process parameters. Infill density, outer shell width, infill pattern, and layer thickness were examined. Taguchi studies tested all parameter values with the fewest possible tests. Infill density 75% affected compressive resistance the most, followed by outer shell width (1.8 mm), infill pattern (75%), infill pattern type (concentric), nozzle diameter (0.6 mm), and layer thickness (0.3 mm) maximum compression strength (55.488 MPa) and the linear regression model which use to prediction experimental value shown minimum percentage error (4%). The study also demonstrated the fabrication of 3D-printed crowns using polylactic acid (PLA) polymer and FDM printing as temporary crowns, which remained intact without any discomfort until the permanent prosthesis was ready. The average printing time for temporary crowns was approximately 7 minutes. This study indicates that 3D printing of temporary crowns with PLA using FDM printing is a convenient process for dentists the result for crowns for teeth 13 and 16 of the human case study showed good accuracy and good resistance to compression.

Keywords: 3D printing, compression, regression model, prediction, crown dental.

INTRODUCTION

A technical test was developed to evaluate the dimensional accuracy and surface roughness of 3D-printed models using various materials and printing processes, which measured the internal and external thread profiles. The study found that Stratasys' ABS-M30 had superior surface quality compared to 3D printers using PLA, ABS, and PETG. Another study discussed the strength of 3D-printed parts and tested DIN EN ISO 527-1:2019 samples, which were FDM-printed from PLA, PETG, and SmartABS. The study examined three print filling levels (10, 30, and 60%) and three filling types (line, mesh, and honeycomb) and tested several printing settings for strength using static tensile testing. The study found that PLA samples with grid filling and filling degrees were the strongest. Infill patterns are used to optimize strength, and 3D-printed parts include interior structures called infill. Infill patterns vary

in stiffness, strength, and function, which can make it challenging for product designers and engineers to determine the best infill pattern for their build, leading to wasted time, material, and performance.

The infill pattern is typically used to enhance or replicate a whole part's mechanical qualities, such as stiffness and rigidity while reducing material, production time, and costs. Lightweight parts are in high demand in the automotive and aerospace sectors due to government regulations and customer preferences. The selection of infill patterns is significantly influenced by the strength-to-weight ratio, with lightweight elements requiring less material and faster printing. Print costs have a more significant impact on manufacturing costs than material costs, as reported by Baich et al. Although some companies use additive manufacturing more frequently, subtractive manufacturing still dominates the production of many series-produced parts due to the time required for

3D printing. Infill designs with acute angles can slow down the print nozzle and extend print time. The mechanical demands of the part also play a crucial role, with a component loaded in several ways requiring a different pattern than one restricted in one direction. Using a pattern that is not aligned with the major stress field can weaken the part. The infill percentage or density affects the mechanical properties of the component, so designers should consider this factor. A full print typically performs better than a print with a density below 100%, although effective printing time must also be taken into account.

Infill patterns play a crucial role in determining the mechanical properties of real-world objects, and engineers and designers must select the most suitable one. Two primary infill patterns exist: 2D and 3D. 2D infill patterns support one dimension on each layer, while 3D infill patterns create homogeneous 3D infill structures that strengthen the component, with most patterns being isotropic and strong in all directions. This article focuses on 2D infill patterns such as Grid, Lines, Triangle, Concentric, Zigzag, Crosses, and Tri-hexagonal, which repeat their pattern layer by layer, occasionally rotating to produce new shapes. Concentric 3D, Cubic, Gyroid, Octet, Tetrahedral, Cross 3D, and Quarter Cubic complete the set of 3D infill patterns studied in this article. Infill patterns vary depending on the slicer program used, with the Slicer program providing more patterns and designs. New designs, often inspired by nature, require further research and are not included in conventional slicer software infill pattern collections. To enhance additive manufacturing, FEA aids infill pattern research by generating infill patterns using projected stress profiles, which may enhance component stiffness while maintaining loads. CAD-designed infill patterns may be the future of fused deposition modeling (FDM) and can improve mechanical characteristics through numerous infill designs. CAD can create bioinspired infill designs, and research is ongoing to improve lattice structures. All of the above are crucial for improving infill patterns, but they are beyond the scope of this research.

THREE-DIMENSIONAL PRINTING IN DENTISTRY

3D printing technology was improved by intraoral scanners, table scans, and

biomaterial-compatible 3D printers. It is used for restoration (permanent and temporary crowns and bridges), physical model preparation, surgical guides, dentures and prostheses, dental implant guides, endodontic guides, patient-specific tissue regeneration scaffolds, and orthodontics. 3D printing allows the creation of complex customized products with intricate details, ease of availability, high precision, and personalized service with increased quality, economics, no biomaterial waste, simplification of the manual workflow with greater accuracy and speed, and efficiency. 3D and 4D imaging technologies in dentistry are the result of medical and health technology research. additive manufacturing-based rapid prototyping approach. It improved microscopic human detail, accuracy, and precision. It collects clinical trial data to encourage evidence-based practices [19]. For Waad Q. ShiaaIn et al. [20] intervention treatments or joint replacement plans, models must be exact and depict the bones' natural appearance. The knee joint relies on femur mobility. Thus, accurately rebuilding the femur model aids joint replacement component design. These models also improve implant design accuracy with accurate measurements. Thus, precise 3D bone tissue models are essential. This research provides a novel method for accurate bone tissue reconstruction from CT data. Histogram modeling, interpolation, and reverse engineering are used. To extract the ROI (bone), soft tissues and artifacts are removed. Using pixel variance from each slice, feature points are retrieved and interpolated to build a 3D point cloud. Point cloud data creates a 3D model. The model is also FDM-printed. To assess its strength and performance, the approach is tested on the femur and sheep bone CT stacks. The suggested technique accurately described bone geometry using feature points. The proposed approach was 1.62% off the actual bone. The proposed strategy yields encouraging results. The 3D bone model matches real bones better. Iveta Katrevaet [21] A patient who has to replace his upper left first and second molar prostheses uses 3D-printed full-coverage provisional crowns and cast patterns for press ceramic crowns. From scanning the imprint to virtual creation, the technique is outlined. 3D printing is fast and precise because it eliminates handwork. Using CAD, the Rapidshare D30 3D printer can make models, ceramic crown molds, and temporary crowns. Stereolithography, is a popular additive technology in dentistry, as compared to conventional crown

production. 3D printing has several benefits. It saves time, structures fit well, there are no lab distortions or errors, sophisticated forms may be made without special equipment or gypsum working models with detachable dies, there is almost no waste material, etc. Eun-Kyong Kim [22] Digital dentistry enhances 3D printing. Fused deposition modeling (FDM) printers are used to make polylactic acid temporary crowns (PLA). Five participants received one full-coverage crown at a university medical center dental clinic from June to August 2022. Temporary crowns were PLA-printed FDM. Users assessed discomfort, breakage, and movement. until reliable implants were available. unbreakable and painless. Temporary crown printing averaged 7 minutes. Dentists make partial crowns quickly with PLA and FDM printers. These crowns are rough and transparent for better 3D printing.

This study explores how the compression strength of 3D printed objects made from PLA filament is affected by various FDM (Fused Deposition Modeling) process parameters. The study appears to focus on the dental industry, as it mentions dental applications.

METHODOLOGY

This paper outlines the experiment’s materials, structures, and compression testing.

Printing parameters and materials

Solidworks created a 3D model. All specimens were produced using the same ENDER 3 settings to ensure consistency in testing, as shown in Figure 1. The printer builds 25×25×25 mm. The Dremel DigiLab 3D Slicer with Ultimaker Cura cut the model. Table 1 shows the test specimen printing settings.

All specimens were printed using Polylactic Acid (PLA).this study’s 27 samples. ASTM D695-15, “Standard Test Method for Compressive Properties of Rigid Plastics,” specifies compression test factors, including maximum compression strength. Instron’s maximum load is 10,000 newtons [23]. 12.7 mm in diameter by 25.4 mm (0.50 by 1 inch) is ideal. Figure 2 shows the mm-scale CAD model. To avoid product system faults, all cylinders were the same size. Figure 2 illustrates test specimen dimensions.

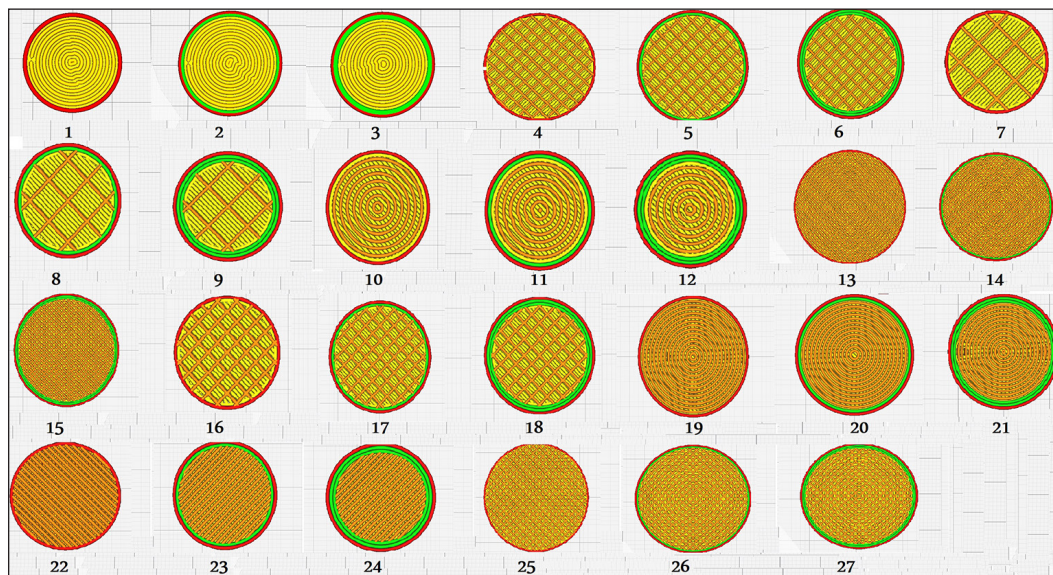


Figure 1. Internal design for 27 samples

Table 1. Testing specimen printing settings

No	Infill	Nozzle dia	Fill pattern	Layer thickness	Shell
1	25	0.4	Line	0.1	1d
2	50	0.6	Concentric	0.2	2d
3	75	0.8	Tringle	0.3	3d

Note: Mat. PLA, printing speed (60 mm/s), nozzle temp. 210 °C, platform temp. 45 °C, all tests were performed at 25 ± 2 °C.

Testing setup

An Instron 5567 machine performed compression tests. Figure 3 shows this study’s compression testing machine. Each test iteration involved repositioning the test cylinders in the same spot. The machine’s ruler also sets the starting height for each test. Extension rate, maximum load, and maximum extension impact compression test results. Table 2 and Figure 3 show the compression test setup and parameters (compression parameters).

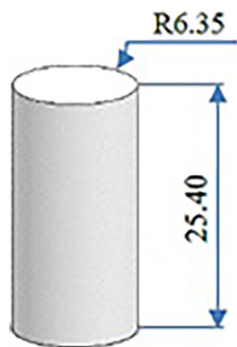


Figure 2. Test specimen with dimensions (mm)

STEP OF THE PROCESS

The practical part represents the design of 27 cylindrical compression samples using the program (Solidworks) and according to the dimensions shown in Figure 2 and stored in STL format to the Cura program, which works on dividing the

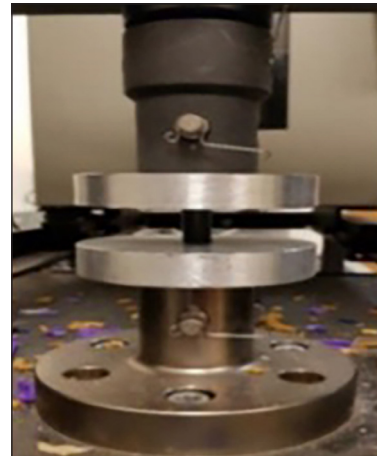


Figure 3. Test setup

Table 2. Compression strength measured, prediction and error

No	Infill density	Nozzle dia	Fill pattern	Layer thickness	Shell	Compressive strength (MPA)	Prediction	Error
1	25	0.4	Concentric	0.1	1d	9.225	7.984	1.241
2	25	0.4	Concentric	0.1	2d	14.997	12.424	2.573
3	25	0.4	Concentric	0.1	3d	17.844	16.864	0.98
4	25	0.6	Liner	0.2	1d	9.924	13.373	-3.449
5	25	0.6	Liner	0.2	2d	16.493	17.813	-1.32
6	25	0.6	Liner	0.2	3d	20.850	22.253	-1.403
7	25	0.8	Tringle	0.3	1d	18.406	18.762	-0.356
8	25	0.8	Tringle	0.3	2d	24.402	23.202	1.2
9	25	0.8	Tringle	0.3	3d	31.540	27.642	3.898
10	50	0.4	Liner	0.3	1d	29.344	29.248	0.096
11	50	0.4	Liner	0.3	2d	34.973	33.688	1.285
12	50	0.4	Liner	0.3	3d	37.263	38.128	-0.865
13	50	0.6	Tringle	0.1	1d	25.533	25.997	-0.464
14	50	0.6	Tringle	0.1	2d	28.876	30.437	-1.561
15	50	0.6	Tringle	0.1	3d	29.939	34.877	-4.938
16	50	0.8	Concentric	0.2	1d	31.435	31.599	-0.164
17	50	0.8	Concentric	0.2	2d	35.905	36.039	-0.134
18	50	0.8	Concentric	0.2	3d	39.421	40.479	-1.058
19	75	0.4	Tringle	0.2	1d	41.194	41.872	-0.678
20	75	0.4	Tringle	0.2	2d	45.74	46.312	-0.572
21	75	0.4	Tringle	0.2	3d	54.433	50.752	3.681
22	75	0.6	Concentric	0.3	1d	46.980	47.474	-0.494
23	75	0.6	Concentric	0.3	2d	50.041	51.914	-1.873
24	75	0.6	Concentric	0.3	3d	55.488	56.354	-0.866
25	75	0.8	Liner	0.1	1d	48.048	44.223	3.825
26	75	0.8	Liner	0.1	2d	48.915	48.663	0.252
27	75	0.8	Liner	0.1	3d	53.248	53.103	0.145

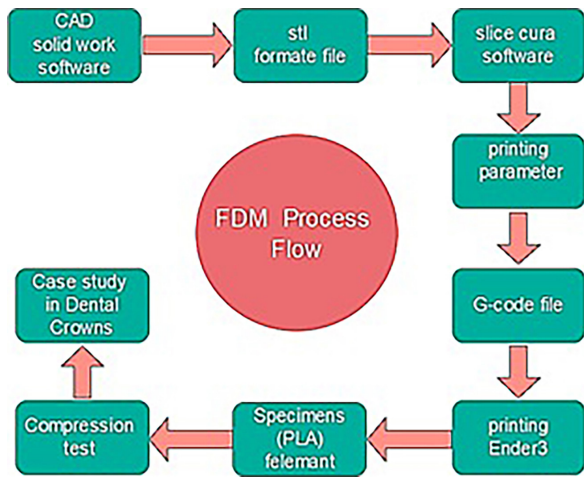


Figure 4. Process Flow chart

design into slices and transferring it to the g-code 3-printer for printing using PLA. Then, the maximum compressive strength was examined using the compression device and the application of the best sample to achieve the maximum conditions of compression with its conditions in the application of crown dental for satisfactory cases. as shown in this step in Figure 4.

Table 2 represents the measured value and the predicted value using the regression model method, and, according to the linear prediction

equation (1), draws the relationship between them according to Figure 5, finding the error for each sample and the total error rate for all samples.

The regression Equation 1 is:

$$\text{compression} = -20.0 + 0.623 (\text{infill density}) + 12.9 (\text{nozzle dia}) - 0.071 (\text{fill pattern}) + 28.8 \text{layer thickness} + 4.44 \text{shell} \quad (1)$$

Table 3 demonstrates that fill density has the greatest effect (rank 1) on effective printing time. Sheel thickness is second, line infill pattern is superior, and nozzle diameter is the least effective (rank 5). Figure 6 shows the signal-to-noise ratios of the primary effects, which may be optimized to reduce specimen printing time.

Figure 7 shows that the concentric infill design has the best compression strength of the five parameters studied. The infill density is the most important component for compression strength, whereas the nozzle diameter is the least important factor for lowering specimen weight. Table 4 shows compression strength and signal-to-noise ratio values. And represent the percentage effect of each parameter in the compression process. As shown in the table, the largest effect parameter in the process is infill density at 70%, and the minimum effect parameter is nozzle diameter at 5%.

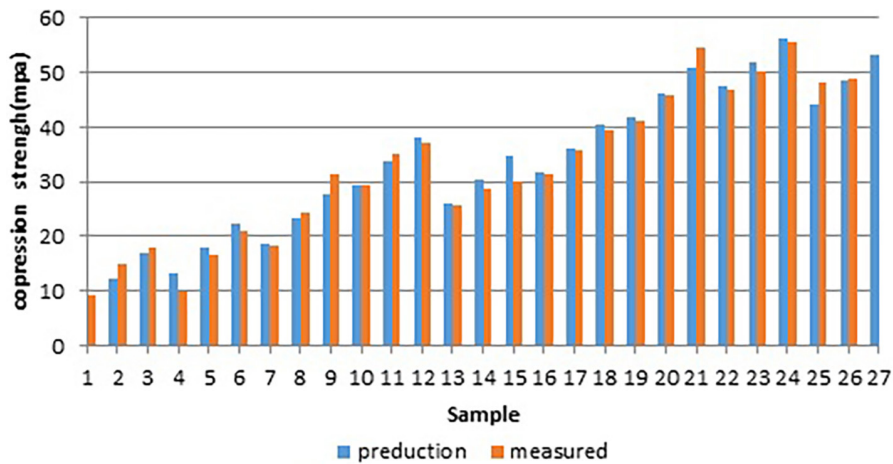


Figure 5. Measured and prediction compressive strength

Table 3. Response for S/N ratio for tensile strength

Level	Infill density	Nozzle diameter	Layer pattern	Shell thickness	Shell
1	24.62	35.52	29.24	28.52	27.93
2	36.83	28.87	36.03	29.32	36.42
3	33.83	30.88	30.01	37.44	30.93
Delta	12.22	6.65	6.79	8.92	8.49
Rank	1	5	4	2	3

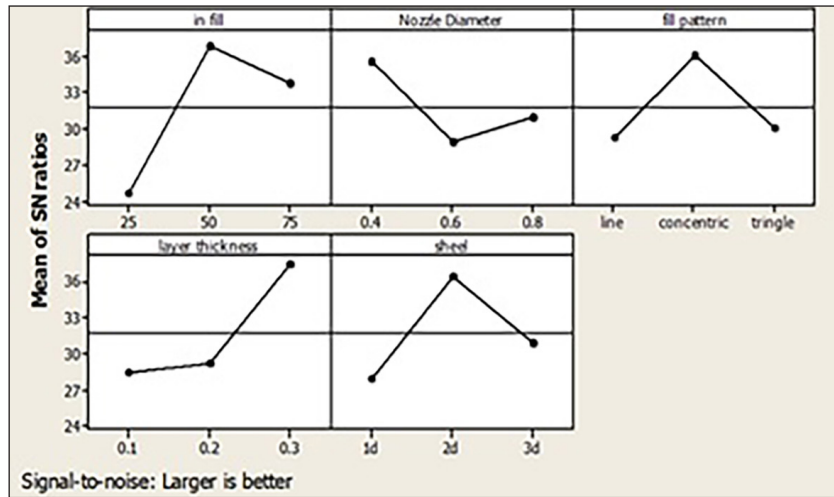


Figure 6. S/N ratio for compression strength

Table 4. Response for S/N ratio for printing time

Source of variance	DOF	Sum of squares	Variance	P (%)
Infill density	2	90366116	45183058	70.19%
Nozzle diameter	2	90302304	45151152	5.25%
Infill pattern	2	90411188	45183058	6.03%
Layer thickness	2	90639439	45319719	10.31%
Shell	2	90366116	45183058	8.09%
Error, e				
Total	18	5097		100%

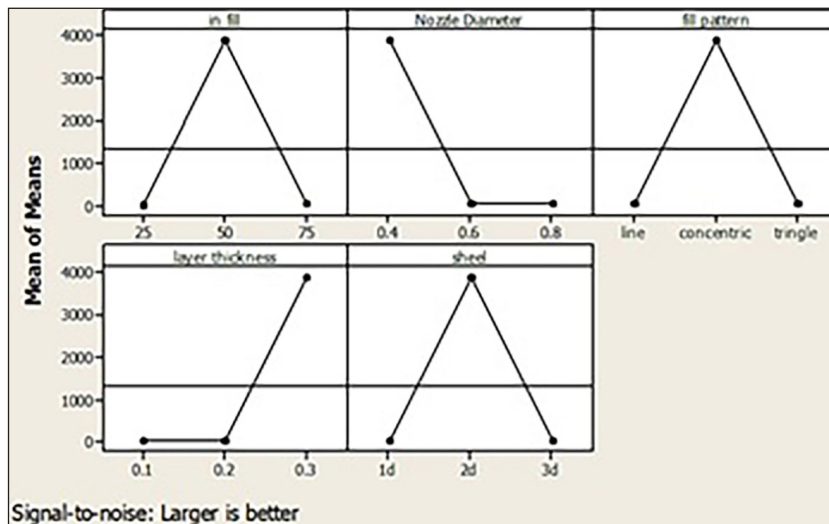


Figure 7. Main effect plot

EXPERIMENTAL WORK

The steps involved in 3D printing are depicted in Figure (8) Techniques of three-dimensional printing in dentistry 3D printing approach broadly employed in dentistry consists of fused deposition modeling.

- first step – using the Smart Optics Vinyl Hi-Resolution 3D Scanner (so-20900)

in the Al-Rahma Laboratory for Dental Technologies.

- second step – Software used for designing the crown tooth using exo-cad (3.1) for design and model creator.
- third step – manufacturing using fused deposition 3D printing Creality ender-3 and (pla) filament.



Figure 8. Steps in three-dimensional printing

3D printing may be utilized in medical applications like bone tissue creation. Our remote control method and understanding of printing material characteristics allow us to simulate multi-material bones. FDM machines printed samples (Creality Ender 3), and 1.75 mm PLA filament was used for printing. Solidworks and Cura samples must be printed. As indicated, to build a 3D printing G-code for a 3D printer, the printing parameter

using the maximum compression strength, which is necessary for human teeth crowns, according to Table 2, was 55.448 MPa in sample no. 24 nozzle diameter of 0.6 mm, shell thickness of 1.8 mm, the printing speed of 90 mm/s, layer thickness of 0.3 mm, infill pattern (concentric), and infill density of 75%.

Patients who visited a dental clinic at Al-Rahma Laboratory for Dental Technologies in Baghdad, Iraq, in May 2022 were chosen as prospective respondents. One example with a single full-coverage restoration was chosen from among five patients. The dental mold or dental model portrays the patient’s teeth and the surrounding

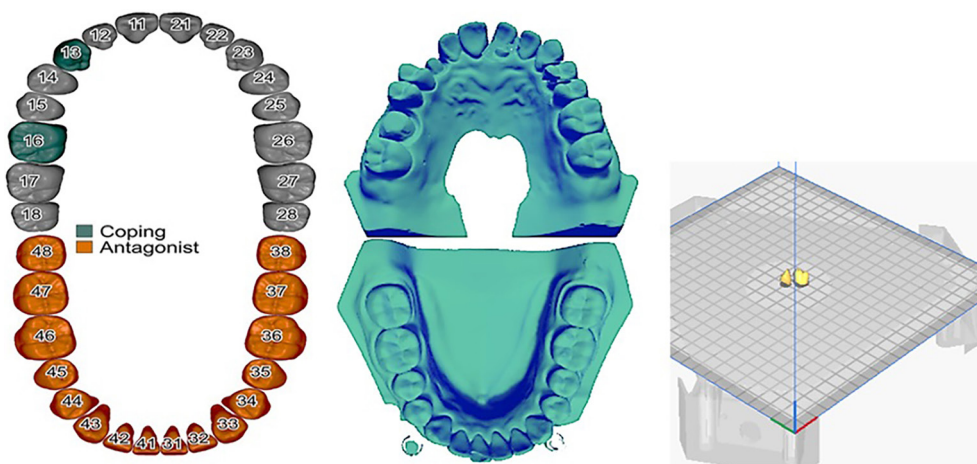


Figure 9. A temporary crown made with PLA using the FDM process



Figure 10. Fabrication of a three-dimensional (3D)-printed temporary crown using the fused deposition modeling method and polylactic acid polymer. (A) Smart Optics Vinyl Hi-Resolution 3D Scanner (B) Nexway PLA. (C) Fabrication of a single temporary crown using PLA. (D) Software used for designing the crown tooth using exo-cad (E) Single temporary crown made with PLA

tissue “gums” produced from the impressive cast. During mastication, a 70-year-old woman complained of pain in teeth 13 and 16. Based on clinical and radiographic evidence, the patient was identified with broken teeth 13 and 16, and he had root canal therapy and core buildup. As shown in Figure (9), To cover the treated tooth, a fused deposition 3D printing crown was developed and prepared. Figure 10 shows a temporary crown made with PLA using the FDM process. After tooth preparation and intraoral scanning with a 3D scanner (Smart Optics Vinyl Hi-Resolution 3D Scanner) in Al-Rahma Laboratory, an additive manufacturing technique were done on the prepared tooth. A 3D-printed temporary crown is created using a digital flow method that includes 3D scanning of the prepared tooth, digitalization on a computer, transfer to a 3D printer, and 3D structure production.

CONCLUSIONS

This article shows the functional connection between process factors and specimen compression strength in medical applications. The optimum parameter for getting maximum compression strength when the nozzle diameter of 0.4 mm, shell thickness of 0.8 mm, the printing speed of 90 mm/s, the layer thickness of 0.3 mm, infill pattern concentric, and infill density of 50%. Maximum compression strength was 55.448 MPa in sample no. 24 with a nozzle diameter of 0.6 mm, shell thickness of 1.8 mm, the printing speed of 90 mm/s, layer thickness of 0.3 mm, infill pattern concentric, and infill density of 75%. The findings demonstrated that anisotropic process parameters greatly impact 3D-printed products' mechanical qualities. Infill density dominates compressive strength (70%), but nozzle diameter has little influence (5%) on compression. The linear regression model prediction equation gives a good correlation with the measured value for compression strength with 96% accuracy. The proposed strategy provides beneficial outcomes. The 3D cover model matches the genuine bone better. 3D printing offers several benefits. It saves time, structures fit well, there are no lab distortions or mistakes, sophisticated shapes may be made without special equipment or gypsum working models with removable dies, and there is almost no waste material. Recommendations use (PETEG) in the 3D printer as a filament material

in dental applications because more acceptable to humans without causing infection or toxicity.

REFERENCES

1. Budzik G. et al. Geometrical Accuracy of Threaded Elements Manufacture by 3D Printing Process. *Advances in Science and Technology Research Journal*. 2022; 16(5): 52–63.
2. Zubrzycki J. et al. Influence of 3D Printing Parameters by FDM Method on the Mechanical Properties of Manufactured Parts. *Advances in Science and Technology Research Journal*. 2023; 17(1): 5–45.
3. Global additive manufacturing market growth 2026. (n.d.). Statista. Retrieved August 11, 2021, from <https://www.statista.com/statistics/284863/additive-manufacturing-projected-global-market-size>.
4. Torres J., Cole M., Owji A., DeMastry Z., Gordon, A. An approach for mechanical property optimization of fused deposition modeling with polylactic acid via the design of experiments. *Rapid Prototyping Journal*. 2016; 22: 387–404. <https://doi.org/10.1108/RPJ-07-2014-0083>
5. Schmitt, M., Mehta, R.M., Kim, I.Y. Additive manufacturing infill optimization for automotive 3D-printed ABS components. *Rapid Prototyping Journal*. 2019; 26(1): 89–99. <https://doi.org/10.1108/RPJ-01-2019-0007>
6. Baich, L., Manogharan, G., Marie, H. 2015. Study of infill print design on production cost-time of 3D printed ABS parts. *International Journal of Rapid Manufacturing*, 5, 308. <https://doi.org/10.1504/IJRAPIDM.2015.074809>
7. Huang, S.H., Liu, P., Mokasdar, A., Hou, L. Additive manufacturing and its societal impact: A literature review. *The International Journal of Advanced Manufacturing Technology*. 2013; 67(5): 1191–1203. <https://doi.org/10.1007/s00170-012-4558-5>
8. Arceo F. 2021. Infill Patterns; Which is the strongest one for 3D printing? 3D Solved. Retrieved August 20, 2021. from <https://3dsolved.com/infill-patterns-which-is-the-strongest-one-for-3d-printing>.
9. Aloyaydi B., Sivasankaran S., Mustafa A. Investigation of infill patterns on the mechanical response of 3D printed poly-lactic acid. *Polymer Testing*. 2020; 87: 106557. <https://doi.org/10.1016/j.polymertesting.2020.106557>.
10. Alvarez K., Lagos R., Aizpun M. Investigating the influence of infill percentage on the mechanical properties of fused deposition modeled ABS parts. *Ingeniería e Investigación*. 2016; 36: 110–116. <https://doi.org/10.15446/ing.investig.v36n3.56610>
11. Infill settings. Ultimaker Support. Retrieved June 14, 2021. 2020. <https://support.ultimaker.com/hc/>

- en-us/articles/360012607079-Infill- settings.
12. Infill patterns. Prusa Knowledgebase. Retrieved June 17, 2021. 2021. https://help.prusa3d.com/en/article/infill-patterns_177130.
 13. Podroužek J., Marcon M., Ninčević K., Wan-Wendner R. Bio-Inspired 3D infill patterns for additive manufacturing and structural applications. *Materials*. 2019; 12(3): 499. <https://doi.org/10.3390/ma12030499>
 14. Gopsill J., Hicks B. Deriving infill design of fused deposition modelled parts from predicted stress profiles. V02AT03A033. 2016. <https://doi.org/10.1115/DETC2016-59935>
 15. Gopsill J.A., Shindler J., Hicks B.J. Using finite element analysis to influence the infill design of fused deposition modeled parts. *Progress in Additive Manufacturing*. 2018; 3(3): 145–163. <https://doi.org/10.1007/s40964-017-0034-y>
 16. Lalegani Dezaki, M., Mohd Ariffin, M.K.A. The effects of combined infill patterns on mechanical properties in FDM Process. *Polymers*. 2020; 12(12): 2792. <https://doi.org/10.3390/polym12122792>
 17. Wu J., Aage N., Westermann R., Sigmund O. Infill optimization for additive manufacturing—approaching bone-like porous structures. *IEEE Transactions on Visualization and Computer Graphics*. 2018; 24: 1127. <https://doi.org/10.1109/TVCG.2017.2655523>
 18. Yu H., Huang J., Zou B., Shao W., Liu J. 2020. Stress-constrained shell-lattice infill structural optimization for additive manufacturing. *Virtual and Physical Prototyping*, 15(1), 35–48. <https://doi.org/10.1080/17452759.2019.1647488>
 19. Rishi Tyagi, et.all. Three-dimensional printing: Fine-tuning of the face of pediatric dentistry. *Journal of Research in Dental Sciences*. 2022.
 20. Waad Q., Shiaa I. et al. A Novel Method Based on Interpolation for accurate 3D reconstruction from CT images. *International Journal of Intelligent Engineering and Systems*. 2023; 16(2): 506–516.
 21. Katreva I., et al. 3D printing – an alternative of conventional crown fabrication: A case report. *Journal of IMAB - Annual Proceeding (Scientific Papers)* April, 2018; 2048–2054.
 22. Eun-Kyong K. et al. Three-dimensional printing of temporary crowns with polylactic acid polymer using the fused deposition modeling technique: a case series journal of Yeungnam Medical Science [Epub ahead of print]. 2022. <https://doi.org/10.12701/jyms.2022.00612.4>
 23. D20 Committee. Test Method for Compressive Properties of Rigid Plastics. ASTM International. 2015. <https://doi.org/10.1520/D0695-15>